Applied Physics Letters PERSPECTIVE scitation.org/journal/apl

Light extraction in tandem organic light emitting diodes

Cite as: Appl. Phys. Lett. **119**, 060504 (2021); doi: 10.1063/5.0057325
Submitted: 19 May 2021 · Accepted: 29 July 2021 ·
Published Online: 11 August 2021

Xiangyu Fu,[1] Shichen Yin,[1] Yi-An Chen,[2] Liping Zhu,[1] Qi Dong,[1] Chih-Hao Chang,[2] and Franky So[1,a)]

AFFILIATIONS

[1]Department of Materials Science and Engineering, North Carolina State University, Raleigh, North Carolina 27606, USA
[2]Walker Department of Mechanical Engineering, University of Texas at Austin, Austin, Texas 78712, USA

[a)]Author to whom correspondence should be addressed: fso@ncsu.edu

ABSTRACT

Since the invention of organic light emitting diodes (OLEDs), great research efforts have been dedicated to improving their efficiency and lifetime. For high-brightness applications, tandem OLED structures have advantages because of the lower current densities required to achieve high brightness. With the successful development of highly efficient charge generation layers, high brightness tandem OLEDs are used in displays and lighting. However, the major challenge for tandem OLEDs is the low light extraction efficiency, because about 50% of the light is trapped inside the device as waveguide modes. In this Perspective, we first review the recent works done on light extraction, analyze different waveguide mode extraction structures, and then identify the key factors determining the extraction efficiencies in tandem OLEDs.

I. INTRODUCTION

The past three decades mark the rapid growth of mobile and large screen displays. Different from its precursor liquid crystal displays (LCDs), OLEDs are self-emissive thin film devices with lower power consumption and higher contrast ratio.[1] With well-developed manufacturing processes, OLEDs have become the mainstream display technology for small-sized displays such as cell phones and smart watches[2] and are a strong contender for large displays such as TVs. Nowadays, OLEDs are also used in lighting,[3] head-mounted display,[4,5] wearable displays,[6] and medical devices.[7,8]

Typical OLEDs consist of a metal electrode, multiple organic layers, and an indium tin oxide (ITO) electrode on a substrate with an active OLED stack thickness less than 200 nm. For display applications, top-emitting OLEDs with a transparent Mg: Ag top electrode are the preferred structure to accommodate for the bottom thin film transistors.[9,10] In a conventional OLED, charge carriers are injected into the emitting layer and form excitons, which relax radiatively to the ground state emitting photons. The ratio of the emitted photons and the injected charge carriers is defined as the external quantum efficiency (EQE), which is a product of the internal quantum efficiency (IQE) and the light extraction efficiency (LEE). With the development of high quantum yield emitters[11,12] with horizontal dipole orientations[13–15] and charge transport layers with low refractive indices,[16,17] the EQE of a single-stack OLED is approaching 40%.[18,19]

Due to the limited current that can be injected into an OLED[20,21] and the efficiency roll-off at high current density,[22,23] single-stack OLEDs are not sufficient to provide high luminance (>2000 cd m^{-2}) output for applications such as lighting,[24] augmented reality display,[25] and other high brightness applications.[26] With multiple OLED stacks interconnected with charge generation layers (tandem OLEDs), the current density required is significantly reduced through multiple photon generation with several OLED units connected in series, resulting in enhancements in the device brightness and operating lifetime.[27–30] Even with various light extraction schemes to extract the internal optical modes as well as a substrate mode, the LEE of a tandem OLED is limited to about 50%.[31–33] In this Perspective, we will analyze the optical modes of tandem OLEDs and discuss how to improve the LEE through light extraction structures.

II. OPTICAL MODES IN TANDEM OLEDs

The light extraction efficiency of an OLED is limited by the optical modes' trapping photons. Because the organic layers ($n \sim 1.8$), the ITO electrode ($n \sim 2$), and the glass substrate ($n \sim 1.5$) all have a higher refractive index than the air, a great fraction of light is trapped in the waveguide and substrate modes due to total internal reflection.[34,35] In an OLED, emitters can also couple energy to the surface plasmon polariton (SPP) modes, which are evanescent waves that propagate along the surface of the metal/organic interface.[36,37] Only

photons emitted within the air cone in the normal direction become useful ("air mode"). The ratio of the air mode relative to all the optical modes is defined as the LEE.

To maximize the LEE, the first step is to maximize the air mode density. For planar OLEDs, this is done by placing the emitting layers at the antinodes of the OLED microcavity, such that the light output is enhanced by the cavity effect.[38] Since the metal electrode is a reflective mirror, the cavity length is determined by the distance from the emitting layer to the metal.[39–42] As the number of stack increases, the emitting layers are further away from the metal, and the cavity effect becomes weaker.[43] Here, we use optical simulation (Setfos) to calculate the mode percentage of a multi-stack bottom-emitting OLED and a top-emitting OLED in Fig. 1. The refractive index of the capping layer is 1.8, and its thickness is 80 nm. The results show that the air mode percentage decreases with the number of OLED stacks with the exception of the single-stack OLED, which has a lower LEE due to the strong SPP loss. For both multi-stack top and bottom emitting devices, the major loss in LEE is due to the waveguide modes. For tandem OLEDs with more than five stacks, the average LEE approaches 20%, slightly higher than the theoretical 15% LEE limit when the cavity effect is neglected.[44]

Since the cavity effect can only moderately improve the LEE of a tandem OLED, additional light extraction structure is needed to recover the trapped modes. From a single-stack OLED to a tandem OLED, the SPP mode percentage drops from over 30% to below 10%, and the waveguide mode becomes the main light trapping channel. For bottom-emitting OLEDs, 41% of the light is trapped in the waveguide mode, and 24% of the light is trapped in the substrate mode; for a top-emitting OLED, the substrate mode is eliminated, and over 60% of the light is trapped in the waveguide mode. Thus, extracting the waveguide modes becomes a key factor determining the extraction efficiency.

III. WAVEGUIDE MODE EXTRACTION

Waveguide modes can be considered as light rays propagating laterally while bouncing between the two electrodes due to reflection at the metal interface and reflection at the ITO/glass interface. A common strategy to extract the waveguide mode is using scattering/diffraction or patterned interfaces to redirect the light such that it propagates along the normal direction of the glass substrate. Due to absorption from the metal electrode, waveguide modes gradually dissipate as heat as they propagate. Therefore, the efficiency of the light extraction structure depends on the number of reflection paths it takes to extract the waveguide modes. Among the different optical structures, corrugated substrate, embedded scattering layer, and micro-lens array (MLA) are commonly used.

A. Corrugated substrate

In an OLED, a corrugated interface can be used for light extraction through random or coherent scattering of the trapped light [Fig. 2(a)].[45] Often a micro-structure or nano-structure replicated from a master mold onto an optical adhesive on a glass substrate through soft-imprinting is used as a substrate for OLED fabrication. The patterning process is inexpensive and scalable, but the surface morphology must be well controlled because any defects could result in leakage current and device failure. Various periodic, quasi-periodic, and random corrugated substrates have been successfully demonstrated in OLEDs, and over 60% LEE has been demonstrated.[46]

The light extraction effectiveness of the corrugation depends on its overlapping with the optical modes.[49] In a single-stack evaporated bottom-emitting OLED, the corrugation is preserved at the metal electrode interface forming a strongly scattering interface. The electric field of the TM waveguide modes and SPP modes both overlap strongly with the corrugated metal, and therefore, they can be extracted by diffraction or scattering. In a tandem OLED, however, the thick organic stacks planarize the corrugation and lower the scattering effect from the metal electrode [Fig. 2(b)].[47,48] Therefore, extraction of both the TM waveguide and SPP modes is not effective. Instead, the extraction of the TE waveguide modes only relies on the corrugated ITO, which

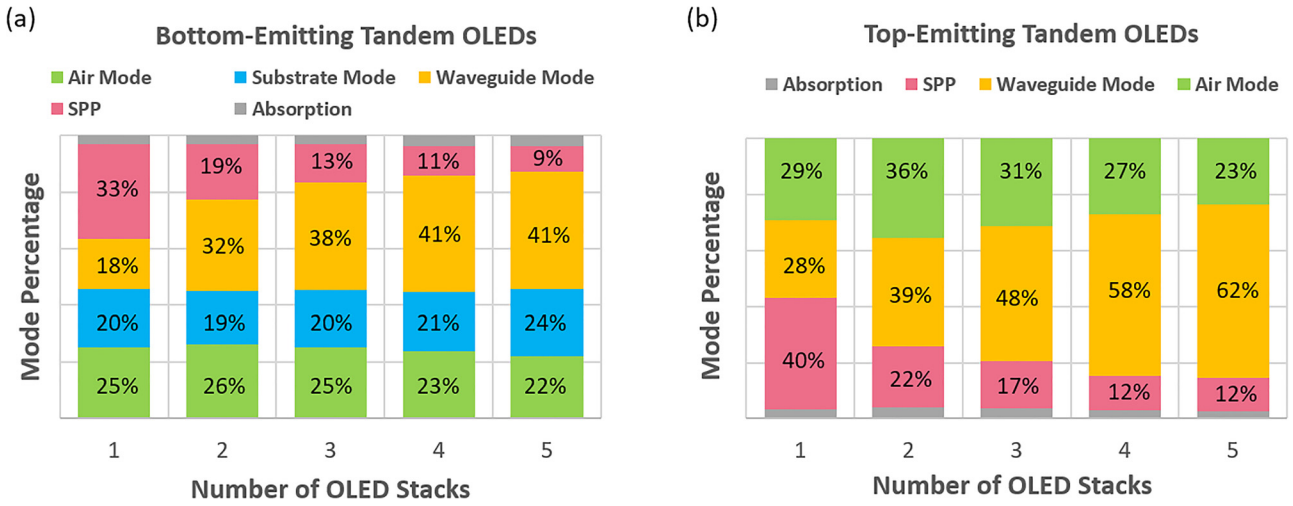

FIG. 1. The percentage of each optical mode in (a) a bottom-emitting OLED (Al/organic/ITO/glass) and (b) a top-emitting OLED (capping layer/thin Mg:Ag/organic/Ag). A single-color emitter (550 nm wavelength) with isotropic emitting dipoles is used for all the simulations in this article. For real emitters, the peak LEE (i.e., air mode percentage) is slightly reduced due to the broader emission spectrum. For emitters with higher horizontal emitting dipole ratio, the peak LEE is higher because more light is emitted toward the substrate normal direction.

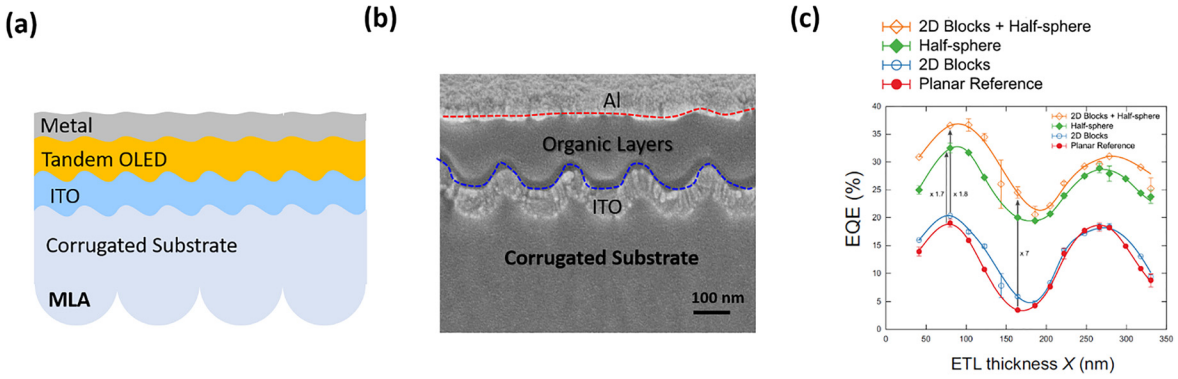

FIG. 2. (a) The structures of tandem bottom-emitting OLEDs fabricated on a corrugated substrate. An external MLA is used for substrate mode extraction. (b) Cross section SEM image of a corrugated OLED. The total thickness of the organic layers is 200 nm. The corrugation depth on the substrate is 100 nm but is reduced to less than 20 nm at the metal electrode. Adapted with permission from X. Fu, Y. Mehta, and Y.-A. Chen, Adv. Mater. **33**(9), 2006801 (2021).[47] Copyright 2021 Wiley-VCH. (c) The influence of the electron transport layer thickness on the EQE of a corrugated OLED patterned with 2D TiO_2 blocks. A half-ball lens is used for extracting the substrate modes. Note the enhancement is lower at the second antinode. Adapted with permission from Will *et al.*, Adv. Funct. Mater. **29**(20) 1901748 (2019).Copyright 2019 Wiley-VCH.

has very limited scattering strength due to the shallow corrugation depth of the ITO electrode, as well as the small index contrast between ITO and the adjacent organic layer and the glass substrate. In general, the light extraction efficiency of the corrugated substrate is lower with thicker organic layers [Fig. 2(c)].[48] To improve the light scattering from the corrugated ITO, a low refractive index layer or embedded air tunnels can be inserted between the ITO and the glass substrate to increase the index contrast.[50]

There are only a handful of reports applying corrugated substrates on tandem OLEDs. Ou *et al.* used quasi-periodic nanocone arrays and demonstrated a 50.4% EQE on a two-stack tandem OLED.[31] The nanocone arrays are fabricated on a spin-coated PEDOT:PSS layer on top of an ITO coated substrate using soft nanoimprint lithography. Li *et al.* demonstrated 76.3% EQE in a two-stack tandem white OLED using a lithography-free patterning approach.[32] The wrinkling pattern can be directly created on the substrate by reactive ions etching (RIE) on poly(dimethylsiloxane) (PDMS), leading to a broad periodicity distribution and an average depth of 150 nm.

For manufacturing, the corrugated substrate fabrication process must be inexpensive and scalable. This rules out high precision patterning techniques such as electron-beam lithography[51] and two-photon photopolymerization.[52] Laser interference lithography[53–56] and holographic interference[57] are effective methods to pattern periodic structures with nanoscale accuracy. However, they are also difficult to scale up, because they usually require sophisticated laser equipment setup and accurate alignment. In addition, most of the techniques discussed above use photoresists as etching masks with low etching selectivity and limited corrugation depth.

Another way to fabricate quasi-periodic structures is by Langmuir–Blodgett assembly of colloidal nanospheres.[58–60] The periodicity can be defined by applying one or multiple sizes of nanospheres.[61] This method can be further introduced to a roll-to-roll system for continuous structures patterning followed by an RIE process for volume fabrication.[62–64] Self-assembled colloidal nanospheres can be made from polymer-based materials such as polystyrene, oxide-based materials such as silicon oxide, and other materials. This process allows the choice of etching mask materials with different etching selectivities and periodicities. Therefore, fine control of nanostructures' geometry is possible. Combining with the roll-to-roll system, Langmuir–Blodgett assembly of colloidal nanospheres might be a method for volume manufacturing with fine control of a nanostructure patterning process.

Random corrugated structures can be fabricated by techniques such as polymer phase separation[65,66] and spontaneous formation through de-wetting[67] or buckling.[68] Among these methods, spontaneously formed buckling patterns can be produced by a thermally evaporating process and does not require further etching process, thus the most suitable for large-area substrate manufacturing.

For effective light extraction, the corrugation geometry is important. While corrugation is effective for single stack OLEDs, its effectiveness for tandem OLEDs is limited. To be effective for light extraction in tandem OLEDs, the corrugation profile must be deep enough for effective light scattering. A deep corrugation profile would lead to device failure, and therefore, a non-planar surface for light extraction for tandem OLEDs is not practical.

B. Embedded scattering layer

Recent research works in light extraction of tandem OLEDs have focused on using planar substrates with embedded light extraction structures to extract the waveguide modes. An embedded scattering layer can be fabricated by starting with a corrugated substrate and then planarizes it with a higher index spacer [Fig. 3(a)]. In this structure, the average refractive index of the embedded scattering layer needs to be the same or higher than the adjacent layer (organic layer and ITO), such that the waveguide modes can be coupled from the OLED stack into the spacer layer for scattering.[69]

To efficiently extract the waveguide modes, the interface of the scattering layer needs to be rough for light incident at large angles to be extracted, and the absorption inside the tandem OLED must be minimized while the emitting light propagating within the OLED stack. For a quantitative analysis, we use 3D ray tracing (Setfos 5.1) to simulate the LEE of tandem OLEDs fabricated on embedded scattering layers [Fig. 3(b)]. We compare different surface roughness root mean square (RMS) of two typical metal electrodes, Al and Ag, which

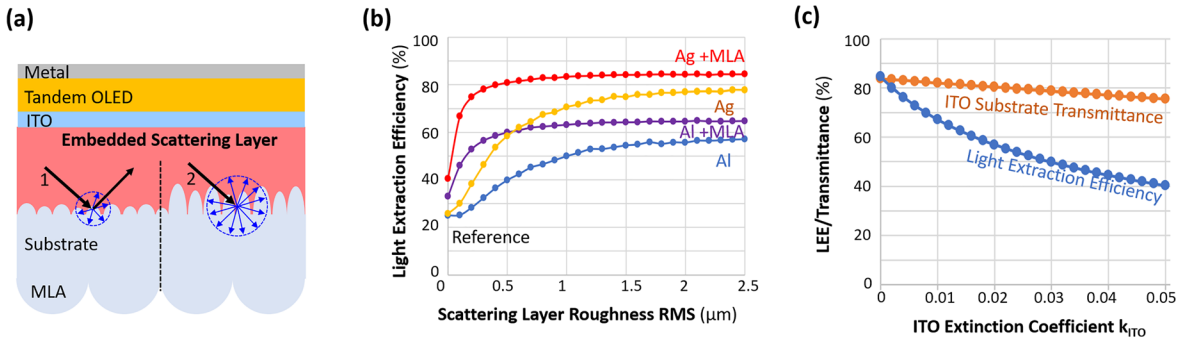

FIG. 3. (a) Schematic drawing of a tandem OLED fabricated on an embedded scattering layer. Two light rays are shown incident on the scattering layer with different surface roughnesses. (b) The dependence of the LEE on the roughness of the scattering layer in a three-stack OLED. Comparisons are made between Al and Ag as the top electrode, and with or without an external MLA. (c) The dependence of the LEE and ITO transmittance on the ITO electrode absorption in a tandem OLED. In tandem OLEDs, the absorption is mainly contributed by the metal and the ITO electrode.

absorbs 15% and 6% of the incident light from an organic layer, respectively.

For tandem OLEDs with an Al cathode, the LEE is improved from 25% to 55% as the RMS increases from 0 to 1.5 μm, which comes from the stronger scattering of the waveguide modes. Further increment in the RMS only improves the LEE marginally toward 58%. When an external MLA is used for extraction, light can more easily escape the substrate, and the LEE is further improved to 63%. Note that after attaching an external MLA, the LEE plateau is reduced from 1 to 0.5 μm. This is because without the external MLA, the scattering strength of the scattering layer needs to be strong enough to extract the substrate mode.

When the top electrode is replaced with Ag, the absorption loss from each reflection on the metal is reduced by more than a half. This greatly extends the lifespan of the waveguide mode, allowing it to have more chances to be extracted by the scattering layer. As a result, the LEE of a tandem OLED without/with the external MLA is improved to 75% and 85%, respectively.

The theoretical 85% peak LEE assumes that light is only absorbed by the metal electrode. In practice, the organic layers, ITO, and a high index spacer also have residual light absorption, which is significant for the waveguide mode, due to its longer lateral propagation length within the OLED. For example, the thickness of the ITO electrode is only 100 nm, but a 1% increase in its extinction coefficient would result in a 15% loss in the LEE while the substrate transmittance is only reduced by 1% [Fig. 3(c)]. This puts a strict requirement on the choice of the high index spacer, which is often over 1 μm thick to efficiently couple the waveguide modes while planarizing the light scattering layer. Furthermore, the fabrication of the embedded scattering layer poses another challenge. To realize the LEE potential, the RMS roughness of the corrugated substrate needs to be larger than 0.5 μm, which would diffuse 90% of the incident light and appear very hazy. Typical processing approaches cannot achieve such a large roughness.

Alternatively, the scattering effect can be improved by increasing the index contrast between the high index spacer ("host") and the low index particles ("dopant"), which often involves introducing voids in an inorganic material. Qu *et al.* fabricated a TiO_2 layer with air grids under the ITO electrode through a combination of photolithography and wafer bonding [Fig. 4(a)].[70] The structure efficiently extracts the waveguide modes without compromising the electrical properties of the OLED. Jeon *et al.* used plasma-enhanced chemical vapor deposition (PECVD) to deposit a high-index Si_3N_4 film and then dry-etched the film to form vacuum nanohole arrays [Fig. 4(b)].[69,72] The structure enhanced the EQE of a single-stack OLED from 20.5% to 78% with a half-full lens attached, owing to the large depth of the vacuum nanoholes. Recently, Han *et al.* demonstrated a more feasible method to

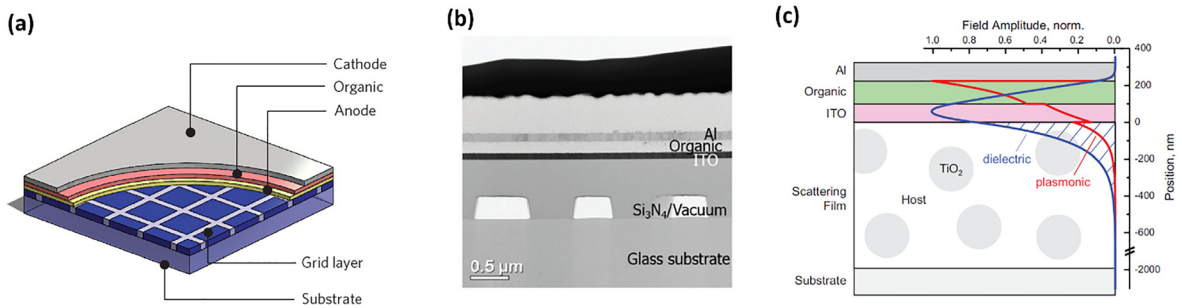

FIG. 4. (a) Schematic cut-away view of an OLED with a sub-anode grid. Reproduced with permission from Qu *et al.*, Nat. Photonics **9**(11), 758–763 (2015). Copyright 2015 Nature Publishing Group. (b) Cross-sectional scanning transmission electron microscopy image of a white OLED fabricated on top of the embedded vacuum nanohole arrays. Reproduced with permission from Jeon *et al.*, "Adv. Opt. Mater. **6**(8), 1701349 (2018). Copyright 2018 Wiley-VCH. (c) Schematic illustration of light extraction in OLEDs by nano-particle based scattering layers. Reproduced with permission from H. Chang, J. Lee, and S. Hofmann, J. Appl. **113**(20), 204502 (2013).[71] Copyright 2013 AIP Publishing.

form hollows inside a TiO_2 spacer by nanoimprinting of a polymer layer and planarizing with TiO_2 nano-particles.[33] During the thermal annealing, the polymer is removed, leaving a hollow nanostructure in the TiO_2 layer. The hollow structure improved the EQE of a two-stack tandem OLED from 82.5% and 103% with the substrate mode extracted by attaching a half-full lens. Nonetheless, processing inorganic materials to form air gaps is not compatible with large-area panel manufacturing.

In comparison, solution processable materials, such as high index polymers, are less expensive and more compatible with roll-to-roll fabrication. Chang *et al.* demonstrated a TiO_2 nano-particle based polymer scattering layer for waveguide mode extraction and achieved 46% EQE in a single-stack OLED with a glass half-ball lens [Fig. 4(c)].[71] Preinfalk *et al.* demonstrated a similar TiO_2/polymer scattering layer on large areas via screen printing.[73] Kim *et al.* fabricated an OLED on top of a polyethylene naphthalate (PEN) substrate, having a high index polymer ($n = 1.7$) filled with organic or inorganic filler particles.[74] The substrate mode and the waveguide mode can be extracted by scattering using filler particles. Despite the potential low-cost processing, the refractive indices of optical polymers are limited to $n < 1.8$ along with residual absorption in the visible range. A summary of the transparent high index materials demonstrated in OLEDs is given in Table I. Some potential high index materials are also listed. Recently, polymeric carbon nitride (pCN), which is transparent in the most visible range, with a high index of 2.27 has been successfully deposited on a large substrate through chemical vapor deposition.[75] However, most of the high index ($n > 1.8$) polymers have an absorption onset at 420–430 nm, which makes these high index polymers unsuitable for OLED light extraction.[76,77] With advances in high index polymer design, we can expect a broader selection of polymers for OLED light extraction.

C. Micro-lens array

High index micro-lens arrays (MLAs) are also used to extract the substrate and waveguide modes [Fig. 5(a)]. A typical MLA has a diameter on the scale of micrometers, much larger than the wavelength of light, and therefore, we can use simple ray tracing to analyze the optics. Because the micro-lens unit is much smaller than an OLED device, light is incident onto the curved MLA surface at random locations, thus reflected/refracted at random angles.

Although the feature-size of an embedded MLA is much larger than an embedded scattering layer, they both function as a scattering layer compared to an OLED device. In Fig. 5(a), we consider a set of parallel light rays incident on a hemispherical MLA from the high index layer. Because a small shift of the incident ray, ray 1 and ray 2 are transmitted/reflected toward different angles, and ray 3 is reflected back toward the metal electrode after several total internal reflections. The average results of random incident angles and sites are similar to random scattering and, thus, can be represented as ray 4.

We simulate the LEE of a tandem OLED fabricated on an embedded MLA and vary the aspect ratios (height/radius) from 0 to 1

TABLE I. List of high refractive index materials used in OLED fabrication.

Host materials	Nano-particles	Refractive index (host/dopant)	Processing	EQE or enhancement	Reference
Si_3N_4	Vacuum	2.02/1.0	PECVD onto nanoimprinted polymer pillar arrays	50% enhancement	78
Si_3N_4	Vacuum	2.02/1.0	Dry-etching the Si_3N_4 PECVD film then anodic bonding the film to glass	78% (with a half-full lens)	69
Zr_2O	MgO	1.84/1.73	E-beam evaporation	34.7% enhancement	79
Resin	SiO_x	1.81/1.5	Nano-coned SiO_X formed by dry-etching	65.3% (with a wrinkle structure to extract substrate mode)	80
[a)]TiO_2	Vacuum	2.0/1.0	Spin-coating TiO_2 NPs and sol onto the thermal-imprinted substrate then anneal at 500 °C	103% (white tandem OLED with a half-full lens)	33
Polymer	TiO_2 NPs	1.5/2.0	TiO_2 NPs dispersed in the monomer solution of polymer and then screen-printing the blend	56% enhancement	73
NOA 73	TiO_2 NPs	1.56/2.0	TiO_2 NPs in NOA 73 and then spin-coating	56%	81
NOA 170		1.7	Spin-coating	37%	82
BDAVBi	···	1.9	Evaporation	NA	77
poly(BTVS)	···	1.74	Spin-coating	NA	83
polymeric carbon nitride (pCN)	···	2.27	Thermal-chemical-vapor-deposition	NA	75
SBDDVE	···	1.91	Sulfur chemical vapor deposition	NA	76

[a)]The TiO_2 is processed from the TiO_2 NPs dispersed resin and TiO_2 sol.

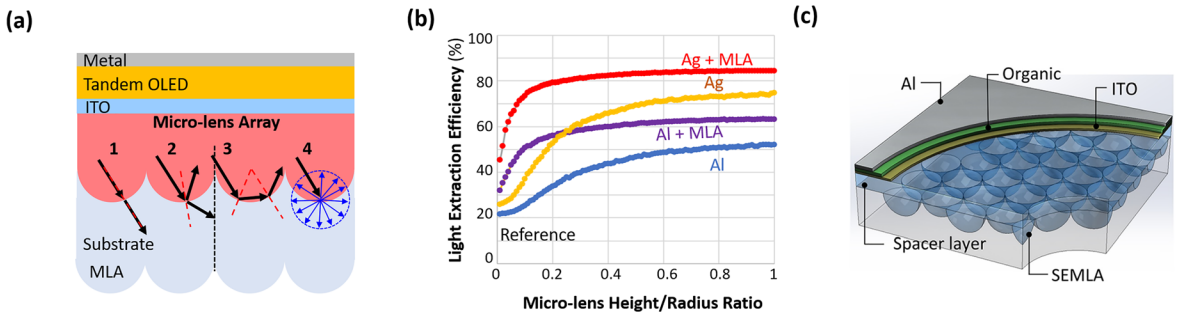

FIG. 5. (a) Schematic drawing of an embedded MLA with hemispherical lens shape for waveguide extraction. Also shown is a set of parallel light rays incident on the embedded MLA at different locations. (b) Dependence of the LEE on the aspect ratio of the MLA. Comparisons are made for Al/Ag electrodes and with/without an external MLA. (c) Schematic illustration of devices on a sub-electrode MLA substrate. Reproduced with permission from Qu *et al.*, ACS Photonics **5**, 2453–2456 (2018).[84] Copyright 2018 American Chemical Society.

[Fig. 5(b)]. Note that the LEE has a very similar dependence on the aspect ratio as on the roughness of a scattering layer. Here, an MLA with a high aspect ratio is better bending the light ray. In addition, when an Ag electrode and an external MLA are used, the LEE can reach 85%, the same value as a scattering layer with over 1 μm roughness RMS.

An MLA index-matched with glass is often used for substrate mode extraction. Reineke *et al.* used a high-index glass substrate with MLAs to extract both the waveguide mode and the substrate mode.[85] However, a high-index glass is costly since containing rare-earth elements.[74] Only recently, Qu *et al.* demonstrated a sub-electrode MLA for waveguide mode extraction [Fig. 5(c)].[84] The sub-electrode layer consists of a polymer spacer layer (NOA 170, n = 1.7) on top of a hexagonal closed-packed array of 10 μm diameter hemispherical MLA. With both an internal and external MLAs, the waveguide and substrate modes are efficiently extracted, leading to a 47% EQE; with an index matching fluid to fully extract the substrate mode, the EQE is further improved to 70%.

D. Light extraction in top-emitting tandem OLEDs

The waveguide mode extraction strategies above apply to top-emitting OLEDs as well, but because the organic thin films are very fragile, the placement of the light extraction structures can be challenging. It also rules out high index materials that require spin-coating or high temperature annealing, which is often used to create embedded scattering layers. In comparison, MLAs can be independently fabricated and attached on the top-emitting OLED [Fig. 6(a)].

Fabricating an MLA on top of an OLED requires special care. Thomschke *et al.* evaporated thin organic on the MLA and then fused it with the OLED device by low temperature annealing.[86] Kim *et al.* evaporated organic materials through a metal mesh with micrometer-size holes to directly form MLAs on an OLED. The shape of the MLA is controlled by the evaporation rate, which offers high aspect ratios for light extraction.[87]

Alternatively, we can use ITO/IZO for both electrodes and embed a reflective light extraction structure under the device [Fig. 6(b)]. Qu *et al.* demonstrated an improved LEE using a reflective sub-electrode grid[88] and then improved the design using a diffusive dielectric reflector to reduce the light absorption.[82] In these two structures, the waveguide modes are scattered randomly at the uneven surfaces, and those scattered light toward the normal direction can be extracted. The advantage of using a spacer structure is compatible with the bottom-up manufacturing of OLED panels. In addition, depending on the scattering strength and the spacer thickness, the waveguide modes can propagate for several micrometers before being extracted, causing

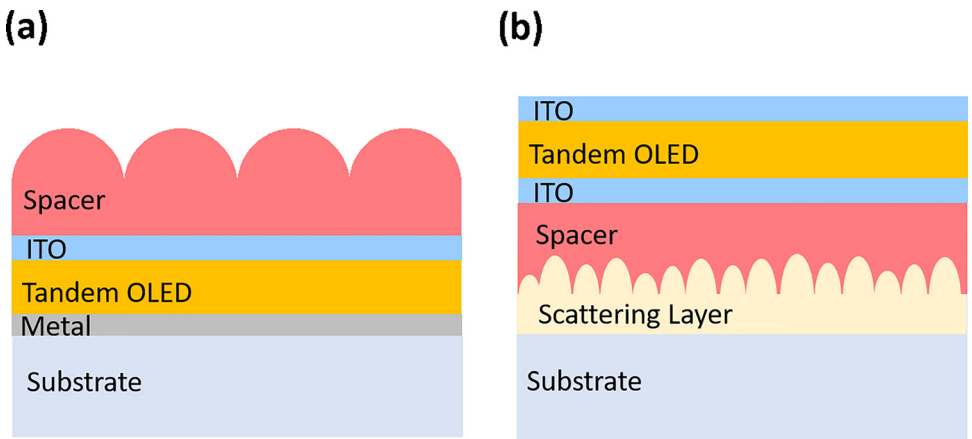

FIG. 6. The structures of tandem top-emitting OLEDs with (a) an MLA on the top spacer and (b) an embedded scattering layer.

haziness from the pixels. In solid-state lightning, haze is not an issue since the OLED panel is orders larger than the spacer thickness; in displays, however, hazy pixels could affect the image quality.

IV. SUMMARY

The pursuit of high efficiency OLEDs remains a challenge, and with the increasing demand for high brightness light sources, tandem OLEDs will be in demand for their performance. In this Perspective, we review the design of tandem OLEDs and the limitation on its light extraction efficiency (LEE) due to strong waveguide mode loss. We then compare different waveguide mode extraction structures including corrugated substrates, embedded scattering layers, and micro-lens arrays, based on a common mechanism of redirecting the trapped light toward the normal direction. We compare the fabrication methods for each structure and conclude that an embedded micro-lens array is the most cost-effective structure for light extraction in large-area OLED panels. Using optical simulation, we identified that the key to achieve high LEEs is to lower the absorption loss using highly transparent and high index materials and to reduce the reflection paths it takes to extract the waveguide mode using light extraction structures with a high aspect ratio. With optimal spacer materials and light extraction structures, the LEE of tandem OLEDs can be enhanced by more than three times. This will significantly reduce the power consumption, making tandem OLEDs the most promising candidate for solid-state lighting and other high brightness applications.

ACKNOWLEDGMENTS

The authors acknowledge the support of the Department of Energy Solid State Lighting program (Award No. DE-FOA-0001823).

DATA AVAILABILITY

The data that support the findings of this study are available within the article.

REFERENCES

[1]H. W. Chen, J. H. Lee, B. Y. Lin, S. Chen, and S. T. Wu, "Liquid crystal display and organic light-emitting diode display : Present status and future perspectives," Light: Sci. Appl. **7**(3), 17168 (2018).
[2]V. C. Coffey, "The age of OLED displays," Opt. Photonics News **28**(11), 34–41 (2017).
[3]Q. D. Ou, L. Zhou, Y. Q. Li *et al.*, "Extremely efficient white organic light-emitting diodes for general lighting," Adv. Funct. Mater. **24**(46), 7249–7256 (2014).
[4]P. Cipresso, I. Alice, C. Giglioli, M. A. Raya, and G. Riva, "The past, present, and future of virtual and augmented reality research: A network and cluster analysis of the literature," Front. Psychol. **9**, 1–20 (2018).
[5]Y.-H. Lee, T. Zhan, and S. T. Wu, "Prospects and challenges in augmented reality displays," Virtual Realilty Intell. Hardware **1**(1), 10–20 (2019).
[6]Y. J. Song, J. Kim, H. Cho *et al.*, "Fibertronic organic light-emitting diodes toward fully addressable, environmentally robust, wearable displays," ACS Nano **14**(1), 1133–1140 (2020).
[7]J. T. Smith, S. Member, B. A. Katchman *et al.*, "Application of flexible OLED display technology to point-of-care medical diagnostic testing," J. Disp. Technol. **12**(3), 273–280 (2016).
[8]Y. Jeon, H. Choi, M. Lim *et al.*, "A wearable photobiomodulation patch using a flexible red-wavelength OLED and its *in vitro* differential cell proliferation effects," Adv. Technol. **3**(5), 1700391 (2018).
[9]C. W. Tang and S. A. VanSlyke, "Organic electroluminescent diodes," Appl. Phys. Lett. **51**(12), 913–915 (1987).
[10]S. Kwon, E.-H. Lee, K. Kim *et al.*, "Efficient micro-cavity top emission OLED with optimized Mg:Ag ratio cathode," Opt. Express **25**(24), 29906 (2017).
[11]S. F. Wu, S. H. Li, Y. K. Wang *et al.*, "White organic LED with a luminous efficacy exceeding 100 l m W−1 without light out-coupling enhancement techniques," Adv. Funct. Mater. **27**(31), 1–9 (2017).
[12]M. Zhang, W. Liu, C. Zheng *et al.*, "Tricomponent exciplex emitter realizing over 20% external quantum efficiency in organic light-emitting diode with multiple reverse intersystem crossing channels," Adv. Sci. **6**(14), 1801938 (2019).
[13]C.-Y. Lu, M. Jiao, W.-K. Lee *et al.*, "Achieving above 60% external quantum efficiency in organic light-emitting devices using ITO-free low-index transparent electrode and emitters with preferential horizontal emitting dipoles," Adv. Funct. Mater. **26**(19), 3250–3258 (2016).
[14]J. Frischeisen, D. Yokoyama, A. Endo, C. Adachi, and W. Brütting, "Increased light outcoupling efficiency in dye-doped small molecule organic light-emitting diodes with horizontally oriented emitters," Org. Electron. **12**(5), 809–817 (2011).
[15]K. H. Kim, S. Lee, C. K. Moon *et al.*, "Phosphorescent dye-based supramolecules for high-efficiency organic light-emitting diodes," Nat. Commun. **5**, 1–8 (2014).
[16]H. Shin, J. H. Lee, C. K. Moon, J. S. Huh, B. Sim, and J. J. Kim, "Sky-blue phosphorescent OLEDs with 34.1% external quantum efficiency using a low refractive index electron transporting layer," Adv. Mater. **28**, 4920–4925 (2016).
[17]C. Fuchs, P.-A. Will, M. Wieczorek *et al.*, "Enhanced light emission from top-emitting organic light-emitting diodes by optimizing surface plasmon polariton losses," Phys. Rev. B **92**, 245306 (2015).
[18]T. Lin, T. Chatterjee, W. Tsai, W. Lee, M. Wu, and M. Jiao, "Sky-blue organic light emitting diode with 37% external quantum efficiency using thermally activated delayed fluorescence from spiroacridine-triazine hybrid," Adv. Mater. **28**(32), 6976–6983 (2016).
[19]T. Watabe, R. Yamaoka, N. Ohsawa, and A. Tomida, "Extremely high-efficient OLED achieving external quantum efficiency over 40% by carrier injection layer with super-low refractive index," in *SID Symposium Digest of Technical Papers* (SID, 2018), Vol. 49, pp. 332–335.
[20]S. Scholz, D. Kondakov, and K. Leo, "Degradation mechanisms and reactions in organic light-emitting devices," Chem. Rev. **115**(16), 8449–8503 (2015).
[21]K. Sawabe, M. Imakawa, M. Nakano, T. Yamao, and S. Hotta, "Current-confinement structure and extremely high current density in organic light-emitting transistors," Adv. Mater. **24**(46), 6141–6146 (2012).
[22]N. C. Giebink and S. R. Forrest, "Quantum efficiency roll-off at high brightness in fluorescent and phosphorescent organic light emitting diodes," Phys. Rev. B **77**(12), 125215 (2008).
[23]C. Murawski, K. Leo, and M. C. Gather, "Efficiency roll-off in organic light-emitting diodes," Adv. Mater. **25**(47), 6801–6827 (2013).
[24]F. So, J. Kido, and P. Burrows, "Organic light-emitting devices for solid-state lighting introduction: The potential for," MRS Bulletin **33**, 663–669 (2008).
[25]Y. Lin, P. Chen, K. Chen *et al.*, "Highly transparent AMOLED for augmented reality applications," in *SID Symposium Digest of Technical Papers* (SID, 2018), pp. 621–623.
[26]J. Song, H. Lee, E. G. Jeong, K. C. Choi, and S. Yoo, "Organic light-emitting diodes: pushing toward the limits and beyond," Adv. Mater. **32**, 1907539:1–17 (2020).
[27]C. W. Chu, C. W. Chen, S. H. Li, E. H. E. Wu, and Y. Yang, "Integration of organic light-emitting diode and organic transistor via a tandem structure," Appl. Phys. Lett. **86**(25), 253503 (2005)
[28]L. S. Liao, K. P. Klubek, and C. W. Tang, "High-efficiency tandem organic light-emitting diodes," Appl. Phys. Lett. **84**(2), 167 (2008).
[29]M. Fung, Y. Li, and L. Liao, "Tandem organic light-emitting diodes," Adv. Mater. **28**(47), 10381–10408 (2016).
[30]P. Xiao, J. Huang, Y. Yu, and B. Liu, "Recent developments in tandem white organic light-emitting diodes," Molecules **24**(1), 151 (2019).
[31]Q. Ou, L. Zhou, Y. Li *et al.*, "Simultaneously enhancing color spatial uniformity and operational stability with deterministic quasi-periodic nanocone arrays for tandem organic light-emitting diodes," Adv. Opt. Mater. **3**(1), 87-94 (2015).
[32]Y. Li, M. Kovac, J. Westphalen *et al.*, "Tailor-made nanostructures bridging chaos and order for highly efficient white organic light-emitting diodes," Nat. Commun. **10**, 2972 (2019).

[33]K. Han, K. Kim, Y. Han *et al.*, "Highly efficient tandem white OLED using a hollow structure," Adv. Mater. Interfaces **7**(9), 1901509 (2020).
[34]M. C. Gather and S. Reineke, "Recent advances in light outcoupling from white organic light-emitting diodes," J. Photon Energy **5**(1), 057607 (2015).
[35]A. Salehi, X. Fu, D. Shin, and F. So, "Recent advances in OLED optical design," Adv. Funct. Mater. **29**, 1808803 (2019).
[36]W. L. Barnes, A. Dereux, and T. W. Ebbesen, "Surface plaston subwavelength optics," Nature **424**(6950), 824–830 (2003).
[37]B. J. Scholz, J. Frischeisen, A. Jaeger, D. S. Setz, T. G. Reusch, and W. Brütting, "Extraction of surface plasmons in organic light-emitting diodes via high-index coupling," Opt. Express **20**(S2), A205 (2012).
[38]T.-Y. Cho, C.-L. Lin, and C.-C. Wu, "Microcavity two-unit tandem organic light-emitting devices having a high efficiency," Appl. Phys. Lett. **88**(11), 111106 (2006).
[39]V. B. Khalfin, G. Gu, and P. E. Burrows, "Weak microcavity effects in organic light-emitting devices," Phys. Rev. B **58**(7), 3730–3740 (1998).
[40]S. Hofmann, M. Thomschke, P. Freitag, M. Furno, B. Lüssem, and K. Leo, "Top-emitting organic light-emitting diodes: Influence of cavity design," Appl. Phys. Lett. **97**, 253308 (2010).
[41]J. Lee, N. Chopra, and F. So, "Cavity effects on light extraction in organic light emitting devices," Appl. Phys. Lett. **92**, 033303 (2008).
[42]J. Lee, T. H. Han, M. H. Park *et al.*, "Synergetic electrode architecture for efficient graphene-based flexible organic light-emitting diodes," Nat. Commun. **7**, 1–9 (2016).
[43]H. Benisty, H. D. Neve, and C. Weisbuch, "Impact of planar microcavity effects on light extraction—Part I: Basic concepts and analytical trends," IEEE J. Quantum Electron. **34**(9), 1612–1631 (1998).
[44]W. Brütting, J. Frischeisen, T. D. Schmidt, B. J. Scholz, and C. Mayr, "Device efficiency of organic light-emitting diodes: Progress by improved light outcoupling," Phys. Status Solidi A **210**(1), 44–65 (2013).
[45]J. M. Lupton, B. J. Matterson, I. D. W. Samuel, M. J. Jory, and W. L. Barnes, "Bragg scattering from periodically microstructured light emitting diodes," Appl. Phys. Lett. **77**(21), 3340–3342 (2000).
[46]W. Youn, J. Lee, M. Xu, R. Singh, and F. So, "Corrugated sapphire substrates for organic light-emitting diode light extraction," ACS Appl. Mater. Interfaces **7**(17), 8974–8978 (2015).
[47]X. Fu, Y. Mehta, and Y.-A. Chen, "Directional polarized light emission from thin-film light-emitting diodes," Adv. Mater. **33**(9), 2006801 (2021).
[48]P. Will, M. Schmidt, K. Eckhardt *et al.*, "Efficiency of light outcoupling structures in organic light-emitting diodes: 2D TiO_2 array as a model system," Adv. Funct. Mater. **29**(20) 1901748 (2019).
[49]N. Danz, D. Michaelis, C. Wächter, N. Danz, D. Michaelis, and C. Wächter, "Light extraction from OLEDs: the waveguide perspective Light exctraction from OLEDs—The waveguide perspective," Proc. SPIE **6475**, 64750J (2007).
[50]Y. S. Shim, J. H. Hwang, C. H. Park, S.-G. Jung, Y. W. Park, and B.-K. Ju, "An extremely low-index photonic crystal layer for enhanced light extraction from organic light-emitting diodes," Nanoscale **8**(7), 4113–4120 (2016).
[51]T. H. P. Chang, M. Mankos, K. Y. Lee, and L. P. Muray, "Multiple electron-beam lithography," Microelectron. Eng. **57–58**, 117–135 (2001).
[52]S. Maruo, O. Nakamura, and S. Kawata, "Three-dimensional microfabrication with two-photon-absorbed photopolymerization," Opt. Lett. **22**(2), 132–134 (1997).
[53]C. V. Shank and R. V. Schmidt, "Optical technique for producing 0.1-μ periodic surface structures," Appl. Phys. Lett. **23**(3), 154–155 (1973).
[54]H. I. Smith, "Low cost nanolithography with nanoaccuracy," Physica E **11**(2–3), 104–109 (2001).
[55]A. Bagal and C.-H. Chang, "Fabrication of subwavelength periodic nanostructures using liquid immersion Lloyd's mirror interference lithography," Opt Lett. **38**(14), 2531–2534 (2013).
[56]Y.-A. Chen, S. V. Naidu, Z. Luo, and C.-H. Chang, "Enhancing optical transmission of multilayer composites using interfacial nanostructures," J. Appl. Phys. **126**(6), 63101 (2019).
[57]M. Campbell, D. N. Sharp, M. T. Harrison, R. G. Denning, and A. J. Turberfield, "Fabrication of photonic crystals for the visible spectrum by holographic lithography," Nature **404**(6773), 53–56 (2000).
[58]N. Denkov, O. Velev, P. Kralchevski, I. Ivanov, H. Yoshimura, and K. Nagayama, "Mechanism of formation of two-dimensional crystals from latex particles on substrates," Langmuir **8**(12), 3183–3190 (1992).
[59]N. D. Denkov, O. D. Velev, P. A. Kralchevsky, I. B. Ivanov, H. Yoshimura, and K. Nagayama, "Two-dimensional crystallization," Nature **361**(6407), 26 (1993).
[60]A. van Blaaderen, R. Ruel, and P. Wiltzius, "Template-directed colloidal crystallization," Nature **385**(6614), 321–324 (1997).
[61]W. H. Koo, W. Youn, P. Zhu, X. H. Li, N. Tansu, and F. So, "Light extraction of organic light emitting diodes by defective hexagonal-close-packed array," Adv. Funct. Mater. **22**(16), 3454–3459 (2012).
[62]X. Li and J. F. Gilchrist, "Large-area nanoparticle films by continuous automated Langmuir–Blodgett assembly and deposition," Langmuir **32**(5), 1220–1226 (2016).
[63]M. Parchine, J. McGrath, M. Bardosova, and M. E. Pemble, "Large area 2D and 3D colloidal photonic crystals fabricated by a roll-to-roll Langmuir-Blodgett method," Langmuir **32**(23), 5862–5869 . (2016).
[64]I.-T. Chen, E. Schappell, X. Zhang, and C.-H. Chang, "Continuous roll-to-roll patterning of three-dimensional periodic nanostructures," Microsyst. Nanoeng. **6**(1), 22 (2020).
[65]K. Tanaka, A. Takahara, and T. Kajiyama, "Film thickness dependence of the surface structure of immiscible polystyrene/poly(methyl methacrylate) blends," Macromolecules **29**(9), 3232–3239 (1996).
[66]B. Jiao, Y. Yu, Y. Dai, X. Hou, and Z. Wu, "Improvement of light extraction in organic light-emitting diodes using a corrugated microcavity," Opt. Express **23**(4), 4055 (2015).
[67]J. W. Shin, D. H. Cho, J. Moon *et al.*, "Random nano-structures as light extraction functionals for organic light-emitting diode applications," Org. Electron. **15**(1), 196–202 (2014).
[68]W. H. Koo, S. M. Jeong, F. Araoka *et al.*, "Light extraction from organic light-emitting diodes enhanced by spontaneously formed buckles," Nat. Photonics **4**(4), 222–226 (2010).
[69]S. Jeon, S. Lee, K. H. Han *et al.*, "High-quality white OLEDs with comparable efficiencies to LEDs," Adv. Opt. Mater. **6**(8), 1701349 (2018).
[70]Y. Qu, M. Slootsky, and S. R. Forrest, "Enhanced light extraction from organic light-emitting devices using a sub-anode grid," Nat. Photonics **9**(11), 758–763 (2015).
[71]H. Chang, J. Lee, and S. Hofmann, "Nano-particle based scattering layers for optical efficiency enhancement of organic light-emitting diodes and organic solar cells," J. Appl. **113**(20), 204502 (2013).
[72]S. Jeon, J. H. Lee, J. H. Jeong *et al.*, "Vacuum nanohole array embedded phosphorescent organic light emitting diodes," Sci. Rep. **5**, 8685 (2015).
[73]J. B. Preinfalk, T. Eiselt, T. Wehlus *et al.*, "Large-area screen-printed internal extraction layers for organic light-emitting diodes," ACS Photonics **4**(4), 928–933 (2017).
[74]E. Kim, H. Cho, K. Kim *et al.*, "A facile route to efficient, low-cost flexible organic light-emitting diodes: Utilizing the high refractive index and built-in scattering properties of industrial-grade PEN substrates," Adv. Mater. **27**(9), 1624–1631 (2015).
[75]P. Giusto, D. Cruz, T. Heil *et al.*, "Shine bright like a diamond: New light on an old polymeric semiconductor," Adv. Mater. **32**(10), 1908140 (2020).
[76]D. H. Kim, W. Jang, K. Choi *et al.*, "One-step vapor-phase synthesis of transparent high refractive index sulfur-containing polymers," Sci. Adv. **6**(28), eabb5320 (2020).
[77]D. Yokoyama, K. Otani, T. Nakayama, and J. Kido, "Wide-range refractive index control of organic semiconductor films toward advanced optical design of organic optoelectronic devices," Adv. Mater. **24**(47), 6368–6373 (2012).
[78]S. Jeon, J.-W. Kang, H.-D. Park *et al.*, "Ultraviolet nanoimprinted polymer nanostructure for organic light emitting diode application," Appl. Phys. Lett. **92**(22), 223307 (2008).
[79]K. Hong, H. K. Yu, I. Lee, K. Kim, S. Kim, and J.-L. Lee, "Enhanced light out-coupling of organic light-emitting diodes: spontaneously formed nanofacet-structured MgO as a refractive index modulation layer," Adv. Mater. **22**(43), 4890–4894 (2010).
[80]K. Lee, J.-W. Shin, J.-H. Park *et al.*, "A light scattering layer for internal light extraction of organic light-emitting diodes based on silver nanowires," ACS Appl. Mater. Interfaces **8**(27), 17409–17415 (2016).

[81]J. Song, K. Kim, E. Kim *et al.*, "Lensfree OLEDs with over 50% external quantum efficiency via external scattering and horizontally oriented emitters," Nat. Commun. **9**, 3207 (2018).
[82]J. Kim, Y. Qu, C. Coburn, and S. R. Forrest, "Efficient outcoupling of organic light-emitting devices using a light-scattering dielectric layer," ACS Photonics **5**(8), 3315–3321 . (2018).
[83]Y. Sato, S. Sobu, K. Nakabayashi, S. Samitsu, and H. Mori, "Highly transparent benzothiazole-based block and random copolymers with high refractive indices by RAFT polymerization," ACS Appl. Polym. Mater. **2**(8), 3205–3214 (2020).
[84]Y. Qu, J. Kim, C. Coburn, and S. R. Forrest, "Efficient, non-intrusive outcoupling in organic light emitting devices using embedded microlens arrays," ACS Photonics **5**, 2453–2456 (2018).
[85]S. Reineke, F. Lindner, G. Schwartz, *et al.*, "White organic light-emitting diodes with fluorescent tube efficiency," Nature **459**(7244), 234–238 (2009).
[86]M. Thomschke, S. Reineke, B. Lüssem, and K. Leo, "Highly efficient white top-emitting organic light-emitting diodes comprising laminated microlens films," Nano Lett. **12**(1), 424–428 (2012).
[87]J. B. Kim, J. H. Lee, C. K. Moon, K. H. Kim, and J. J. Kim, "Highly enhanced light extraction from organic light emitting diodes with little image blurring and good color stability," Org. Electron. **17**, 115–120 (2015).
[88]Y. Qu, C. Coburn, D. Fan, and S. R. Forrest, "Elimination of plasmon losses and enhanced light extraction of top-emitting organic light-emitting devices using a reflective subelectrode grid," ACS Photonics **4**(2), 363–368 (2017).